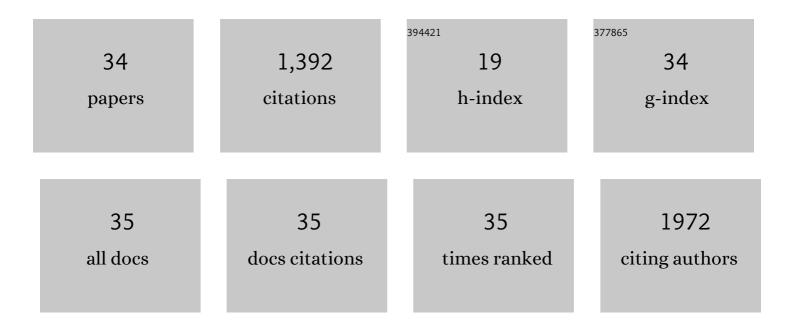
Zhen J Wang

List of Publications by Year in descending order

Source: https://exaly.com/author-pdf/3384632/publications.pdf Version: 2024-02-01



ZHEN LMANC

#	Article	IF	CITATIONS
1	Bosniak Classification of Cystic Renal Masses, Version 2019: An Update Proposal and Needs Assessment. Radiology, 2019, 292, 475-488.	7.3	278
2	Hyperpolarized ¹³ C MRI: State of the Art and Future Directions. Radiology, 2019, 291, 273-284.	7.3	210
3	Hyperpolarized 13C-Pyruvate Magnetic Resonance Reveals Rapid Lactate Export in Metastatic Renal Cell Carcinomas. Cancer Research, 2013, 73, 529-538.	0.9	95
4	Metabolic Reprogramming and Validation of Hyperpolarized ¹³ C Lactate as a Prostate Cancer Biomarker Using a Human Prostate Tissue Slice Culture Bioreactor. Prostate, 2013, 73, 1171-1181.	2.3	93
5	Renal Cyst Pseudoenhancement at Multidetector CT: What Are the Effects of Number of Detectors and Peak Tube Voltage?. Radiology, 2008, 248, 910-916.	7.3	65
6	The Role of 18F-FDG PET/CT and PET/MRI in Pancreatic Ductal Adenocarcinoma. Abdominal Radiology, 2018, 43, 415-434.	2.1	60
7	Noninvasive In Vivo Imaging of Diabetes-Induced Renal Oxidative Stress and Response to Therapy Using Hyperpolarized 13C Dehydroascorbate Magnetic Resonance. Diabetes, 2015, 64, 344-352.	0.6	59
8	Hyperpolarized [1- ¹³ C]Dehydroascorbate MR Spectroscopy in a Murine Model of Prostate Cancer: Comparison with ¹⁸ F-FDG PET. Journal of Nuclear Medicine, 2013, 54, 922-928.	5.0	50
9	Realâ€ŧime measurement of hyperpolarized lactate production and efflux as a biomarker of tumor aggressiveness in an MR compatible 3D cell culture bioreactor. NMR in Biomedicine, 2015, 28, 1141-1149.	2.8	43
10	CT and MRI of small renal masses. British Journal of Radiology, 2018, 91, 20180131.	2.2	39
11	Early Response Assessment in Pancreatic Ductal Adenocarcinoma Through Integrated PET/MRI. American Journal of Roentgenology, 2018, 211, 1010-1019.	2.2	30
12	Blockchain-Authenticated Sharing of Genomic and Clinical Outcomes Data of Patients With Cancer: A Prospective Cohort Study. Journal of Medical Internet Research, 2020, 22, e16810.	4.3	29
13	Hyperpolarized ¹³ C magnetic resonance evaluation of renal ischemia reperfusion injury in a murine model. NMR in Biomedicine, 2017, 30, e3765.	2.8	27
14	Non-Invasive Differentiation of Benign Renal Tumors from Clear Cell Renal Cell Carcinomas Using Clinically Translatable Hyperpolarized 13C Pyruvate Magnetic Resonance. Tomography, 2016, 2, 35-42.	1.8	26
15	Multiparametric Functional Magnetic Resonance Imaging for Evaluating Renal Allograft Injury. Korean Journal of Radiology, 2019, 20, 894.	3.4	23
16	Non-Invasive Assessment of Lactate Production and Compartmentalization in Renal Cell Carcinomas Using Hyperpolarized 13C Pyruvate MRI. Cancers, 2018, 10, 313.	3.7	22
17	Dual Energy Computed Tomography Scans of theÂBowel. Radiologic Clinics of North America, 2018, 56, 805-819.	1.8	21
18	3D T2-weighted and Gd-EOB-DTPA-enhanced 3D T1-weighted MR cholangiography for evaluation of biliary anatomy in living liver donors. Abdominal Radiology, 2017, 42, 842-850.	2.1	20

ZHEN J WANG

#	Article	IF	CITATIONS
19	Imaging glutathione depletion in the rat brain using ascorbate-derived hyperpolarized MR and PET probes. Scientific Reports, 2018, 8, 7928.	3.3	20
20	Separation of extra- and intracellular metabolites using hyperpolarized 13C diffusion weighted MR. Journal of Magnetic Resonance, 2016, 270, 115-123.	2.1	19
21	ACR Appropriateness Criteria \hat{A}^{\circledast} Indeterminate Renal Mass. Journal of the American College of Radiology, 2020, 17, S415-S428.	1.8	19
22	<scp>Wholeâ€Abdomen</scp> Metabolic Imaging of Healthy Volunteers Using Hyperpolarized [<scp>1â€¹³C</scp>]pyruvate <scp>MRI</scp> . Journal of Magnetic Resonance Imaging, 2022, 56, 1792-1806.	3.4	19
23	Multi-institutional analysis of CT and MRI reports evaluating indeterminate renal masses: comparison to a national survey investigating desired report elements. Abdominal Radiology, 2018, 43, 3493-3502.	2.1	18
24	Non-invasive detection of divergent metabolic signals in insulin deficiency vs. insulin resistance inÂvivo. Scientific Reports, 2018, 8, 2088.	3.3	18
25	Hyperpolarized 13C Spectroscopic Evaluation of Oxidative Stress in a Rodent Model of Steatohepatitis. Scientific Reports, 2017, 7, 46014.	3.3	15
26	Therapeutic response assessment in pancreatic ductal adenocarcinoma: society of abdominal radiology review paper on the role of morphological and functional imaging techniques. Abdominal Radiology, 2020, 45, 4273-4289.	2.1	15
27	Lexicon for renal mass terms at CT and MRI: a consensus of the society of abdominal radiology disease-focused panel on renal cell carcinoma. Abdominal Radiology, 2021, 46, 703-722.	2.1	15
28	Adult living donor liver imaging. Diagnostic and Interventional Radiology, 2016, 22, 207-214.	1.5	11
29	Improved Sensitivity and Reader Confidence in CT Colonography Using Dual-Layer Spectral CT: A Phantom Study. Radiology, 2020, 297, 99-107.	7.3	10
30	Specialized computational methods for denoising, B 1 correction, and kinetic modeling in hyperpolarized 13 C MR EPSI studies of liver tumors. Magnetic Resonance in Medicine, 2021, 86, 2402-2411.	3.0	6
31	Protocol Optimization for Renal Mass Detection and Characterization. Radiologic Clinics of North America, 2020, 58, 851-873.	1.8	6
32	Modeling hyperpolarized lactate signal dynamics in cells, patientâ€derived tissue slice cultures and murine models. NMR in Biomedicine, 2021, 34, e4467.	2.8	5
33	Bowel Peristalsis Artifact on Dual-Energy CT: In Vitro Study on the Influence of Different Dual-Energy CT Platforms and Enteric Contrast Agents. American Journal of Roentgenology, 2022, 218, 290-299.	2.2	5
34	Hyperpolarized Carbon (13C) MRI of the Kidneys: Basic Concept. Methods in Molecular Biology, 2021, 2216, 267-278.	0.9	1